



ELSEVIER

Available online at www.sciencedirect.com

Physics Procedia 10 (2010) 94–98

**Physics
Procedia**

www.elsevier.com/locate/procedia

3rd International Symposium on Shape Memory Materials for Smart Systems

Giant two-way shape memory effect in high-temperature Ni-Mn-Ga single crystal

V. A. Chernenko^{a,b}, E. Villa^c, S. Besseghini^c, J.M. Barandiaran^{a,*}^a *Universidad del País Vasco, Dpto. Electricidad y Electronica, P.O. Box 644, Bilbao 48080, Spain*^b *Ikerbasque, Basque Foundation for Science, Bilbao 48011, Spain*^c *CNR-IENI, C.Promessi Sposi, 29, Lecco 23900, Italy*

Abstract

A perfect two-way shape memory effect (TWSME) with reversible strain of about 9% has been found in the high-temperature Ni_{57.5}Mn_{22.5}Ga_{20.0} single crystal transforming into 2M non-modulated martensitic phase. Two thermal/mechanical treatment routes were utilized in the experimental procedures. The outstanding high-temperature TWSME is observed as a result of tensile stress-strain cycling along <100> axis involving huge superelastic strains due to stress-induced martensitic transformation. It is argued that the TWSME is related to the anisotropic internal stresses produced by a network of lattice defects. The defects are generated in the course of oriented growth/shrinkage of the dominating martensitic variant in the tensile sample.

© 2010 Published by Elsevier Ltd. Open access under [CC BY-NC-ND license](http://creativecommons.org/licenses/by-nc-nd/3.0/).*Keywords:* high-temperature Ni–Mn–Ga Heusler alloy; two-way shape memory effect; stress-strain cycling

1. INTRODUCTION

Early works have shown that Ni-Mn-Ga Heusler alloys exhibit a well-pronounced thermal shape memory effect and superelasticity alongside the ferromagnetic shape memory effect (see, e.g., [1-4] and references therein). It was recognized recently that the former two functional abilities can be interesting for the applications in the high temperature range because these alloys, depending on the compositions, exhibit a high-temperature low-hysteresis thermoelastic martensitic transformation (MT) up to about 500°C [5-13].

A reversible spontaneous shape change of the sample during its thermal cycling through MT, known as a two-way shape memory effect (TWSME), is typical for traditional shape memory alloys [14]. The mechanism of this effect is conventionally attributed to the existence of the anisotropic internal stress in the cubic phase which intensity and reproducibility depend on the sample microstructure. The latter is controlled by the processing factors during the alloy production and/or its particular thermomechanical treatment (training). TWSME induced by training was first observed in a polycrystalline Ni-Mn-Ga alloy in Ref.[1]. Later on, this effect was observed as a result of growth conditions in Ni-Mn-Ga polycrystalline thin films and bulk single crystals [15-17]. On the other hand, the thermomechanical training did not assist the formation of TWSME in a single crystalline Ni-Mn-Ga alloy transforming into the modulated martensite [18], whereas the single crystalline samples of Ni-Mn-Ga exhibiting a

* Corresponding author. Tel.+34-946012549

E-mail address: manub@we.lc.ehu.es

non-modulated martensitic structure, indeed, demonstrated significant amounts of TWSME strain of 3.8 % (60% of the theoretical one) after thermal cycling under high compressive stress [19].

In the present work, we studied the exceptional case of the high-temperature behavior of a Ni-Mn-Ga single crystal exhibiting a record-breaking TWSME of about 9% in the vicinity of 300°C. The generation of such result was possible due to the use of tensile training procedures not considered before for this purpose. Some phenomenological ideas are put forward to distinguish between thermal and mechanical training involved.

2. EXPERIMENTAL PROCEDURES

The experiments have been carried out using an oriented single crystal $\text{Ni}_{57.5}\text{Mn}_{22.5}\text{Ga}_{20.0}$ (in at.%, according to X-ray fluorescent analysis) exhibiting a 2M non-modulated martensite with lattice parameters $a=0.543$ nm and $c=0.665$ nm, $c/a = 1.22$. The MT transformation temperatures and transformation heat have been determined by a standard differential calorimeter to be $T_m = 312^\circ\text{C}$, $T_a = 361^\circ\text{C}$ and $q \approx 10\text{J/g}$, respectively.

Two [100]-oriented tensile samples measuring 0.57×0.19 mm² in a cross-section and 9.1 mm as a gauge length (sample A1) and 0.28×0.27 mm²; 7.0 mm (sample A2) were spark cut. They were electropolished to remove the deformed surface layer. A TA Instruments Q800 dynamic mechanical analyzer (DMA) was used in the tensile stress-controlled mode: (a) to perform a cycling of the superelastic loops at constant temperatures, T_{exp} , and to record strain versus temperature curves in quasi-static regime, and (b) to measure the temperature dependence of the low-frequency elastic modulus and internal friction, $\tan\delta$, in the dynamic regime. The same sample was used in these measurements.

In the static mechanical tests, the upper limit of load and the stress change rate were 18 N and 2.5 MPa/min, respectively. The temperature change rate during heating/cooling ramps of strain was $10^\circ\text{C}/\text{min}$ which was optimal to study cycling properties. The $E(T)$ and $\tan\delta(T)$ measurements were carried out at a frequency of 1 Hz and oscillation strain amplitude of 10^{-4} . The temperature change rate was $5^\circ\text{C}/\text{min}$. Further details of the dynamic method can be found elsewhere [26]. Note, that in the DMA measuring unit, the thermocouple is not in contact with the sample. That yields some shift between the temperature of sample and the recorded one [20]. Despite some ambiguity in the values of absolute temperatures, the relative difference between MT temperatures between samples observed in DMA measurements is reproducible and can be commonly attributed a slight variation of the alloy composition in the virgin single crystal.

Two training routes corresponding to the two samples were used to study the TWSME and elastic properties. Route 1 incorporated a recording of the $E(T)$ curve for A1, holding at 400°C for 10 min, then subjecting it to a stress-strain, σ - ε , superelastic cycle at each constant temperature T_{exp} . T_{exp} was step-wise shifted from 400°C to room temperature. After each test, the strain was monitored during stress-free heating to 400°C , holding at such temperature during 10 min and subsequent cooling to the next desired temperature T_{exp} . In total, 15 σ - ε cycles were performed. Route 1 ended with recording $E(T)$ dependence.

Route 2 training procedure started by documenting the $E(T)$ curve for sample A2. Then, 10 σ - ε cycles were recorded at three temperatures T_{exp} between 400°C and T_a , with intermediate annealing at 400°C for 10 min after each series. Afterwards, sample A2 was subjected to 10 heating-cooling cycles through MT under different constant loads up to 100 MPa. $E(T)$ measurement was finally repeated.

3. RESULTS AND DISCUSSION

The stress-strain measurements at constant different temperatures for the sample A1 collected along Route 1 can be found elsewhere [21]. These data yield a huge and reproducible superelastic strain of about 9% persisting up to 400°C , in austenite, and almost the same deformation accumulated in the martensitic state [21]. In the present work, an emphasis is paid to the TWSME exhibited by the same crystal.

The temperature change of the deformation stored by the martensitic phase during straining of sample A1 is shown in Fig. 1. Fig. 1 reveals a perfect shape recovery of the sample contracting by 9% during heating through reverse MT. The prominent feature of the cooling ramps in Fig.1 is a significant spontaneous elongation of sample in the course of the forward MT which amounts to about one-third of the full martensitic strain. This effect is observed just after the first thermal recovery of the full strain. Thus, the appearance of the partial TSME is the main effect of training Route 1. The other consequence is the change in the elastic behavior and transformation

temperatures as can be deduced from Fig. 2. Whereas the non-modulated martensites of single crystalline Co-Ni-Ga and Fe-Ni-Ga-Co alloys are prone to a stabilization effect [22,23], this effect is not the case for Ni-Mn-Ga martensite because no increase of T_a is observed in Fig.1. On the contrary, the training procedures performed during our experiments lead to a decrease of the characteristic MT temperatures as it is clearly seen in Figs. 2-4. Fig. 2 yields this decrease to be about 25°C. An increase of the critical stress σ_c^{ms} as a function of cycle number deduced from Figs. 3 and 4 is also equivalent to a reduction of MT temperature. Such a behavior has been analysed in the

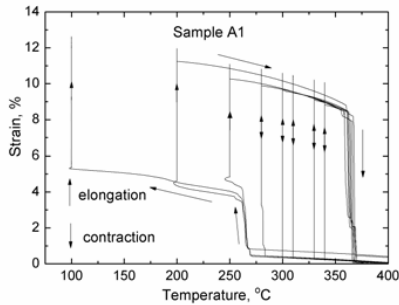


Fig. 1. Stress-free heating-cooling strain showing perfect thermal recovery (contraction) and partial two-way SME (elongation) of the sample A1 trained according to Route 1. The curves were recorded during heating from T_{exp} to 400°C after each $\sigma-\epsilon$ test and subsequent cooling to the next temperature T_{exp} . The loading/unloading tracks of the $\sigma-\epsilon$ tests are shown as vertical lines at the positions of T_{exp} .

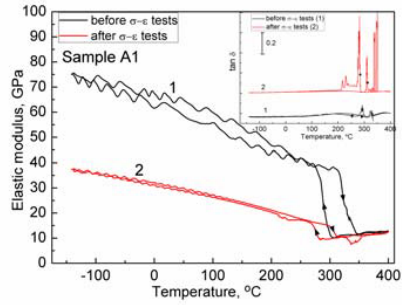


Fig.2. Temperature evolutions of the elastic modulus and $\tan \delta$ of sample A1 in the initial state (1) and after training along Route 1 (2). The serration of curves is an instrumental effect.

framework of a phenomenological model of martensite destabilization (rejuvenation) effect [21,24] which is opposite to the well-known martensite stabilization. In short, the thermal/tensile training procedures give rise to two opposite tendencies: (i) a destabilization of the martensitic structure as a whole due to the uniform dilatation of the crystal lattice by the isotropically introduced defects (resulting in a decrease of the MT temperatures) and a (ii) stabilization of the favorable martensitic variant at the expense of the others, due to the internal uniaxial stress

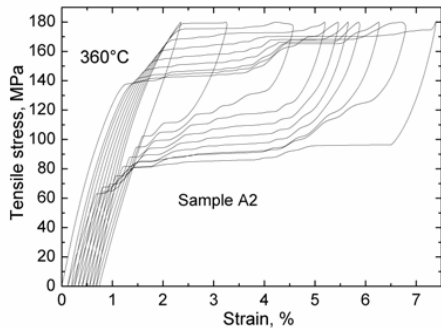


Fig. 3. The $\sigma-\epsilon$ superelastic cycling of sample A2 at 360C showing a strong upward shift of the hysteresis loops as a function of cycle number.

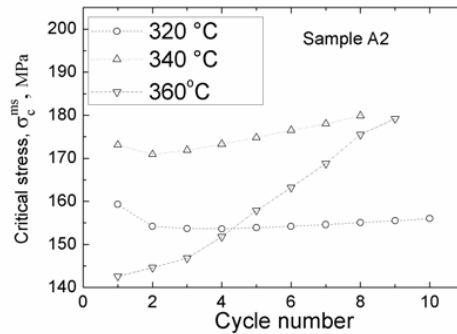


Fig. 4. Critical stress versus cycle number for sample A2 at different temperatures.

produced by a network of oriented lattice defects (resulting in the increase of MT temperatures of this particular variant). The thermal cycling of the loaded or unloaded sample through the MT seems to be more effective to assist the first mechanism (i), initiated by self-accommodating twinning groups, whereas the superelastic σ - ε cycling obviously favours the mechanism (ii). In our experiments, a dominating effect of the first mechanism in the lowering of MT temperatures can be anticipated. This is also corroborated by the results depicted in Figs.5 and 6. According to Fig.6, a drastical decrease of MT temperatures of sample A2 by about 80°C is observed after the treatment within training Route 2 such as shown in Fig. 5. On the other hand, the more “gentle” treatment of sample A1 resulted in a less pronounced reduction of the MT temperatures (of about 25°C, Fig.2). Incidentally, the data in Fig.5 show a conspicuous ability of high-temperature Ni-Mn-Ga to produce a large work output per unit volume during heating under load, estimated about $(5 - 9) \cdot 10^6 \text{ J/m}^3$.

A comparison of the results in Figs.1 and 5 provides clear evidence of the crucial role of the superelastic cycling in the giant TWSME in the high-temperature Ni-Mn-Ga single crystal. Such a mechanical training seems to be a key point to set the same effect in the other Heusler ferromagnetic shape memory materials. So, it is natural to assume that this type of mechanical treatment contributes chiefly to the creation of the thermodynamically stable network of oriented defects which guides the preferential growth of a single variant in the sample during cooling through MT (see also Ref.[21]). The preferred formation of a single variant of martensite and an enhanced interface mobility is supported by the results in Figs. 2 and 6 where a drastic reduction of the effective elastic modulus, accompanied by the increase of $\tan\delta$, is observed in the martensitic phase of the trained samples. The similar effects have been observed when an external stress, higher than the detwinning one, was applied to a 2M-martensite exhibited by Ni-Mn-Ga single crystal studied in Ref.[25]. In both cases, the elevated values of the elastic modulus of the martensite formed in virgin samples suggest a self-accommodated dense twin structure which is normally observed for the aged martensites [19]. On the contrary, a reduced elastic modulus must be typical of rejuvenated martensite, characterized by a coarse twin structure, increased number of defects and large internal stresses. Such a state can be obtained, in particular, in the course of training, such as the one used in the present work. The direct observations of microstructure and its changes would be definitive to confirm the above speculations but in the present work such observations were hindered by the small size of the samples. High temperatures also add a big challenge for possible in-situ microstructural studies to be made in the future.

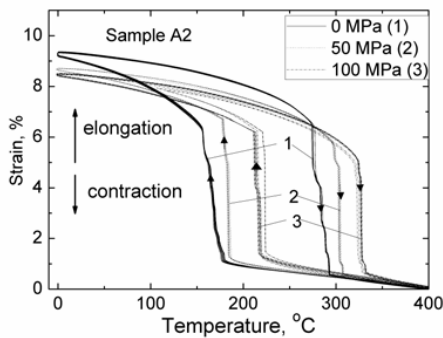


Fig. 5. Strain versus temperature exhibited by sample A2 after training through Route 2. Each curve was measured 10 times. The giant TWSME is observed in curve 1. Curves 2 and 3, measured under the tensile stresses shown in the legend, demonstrate large recovery stresses. For a better comparison, the curves have been shifted to merge at 400°C.

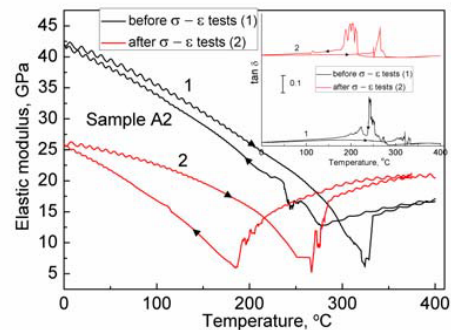


Fig. 6. Temperature dependence of the elastic modulus and $\tan \delta$ of sample A2 in the initial state (1) and after training through Route 2 (2).

In summary, a $\text{Ni}_{57.5}\text{Mn}_{22.5}\text{Ga}_{20.0}$ single crystal exhibiting high-temperature cubic-tetragonal MT ($c/a > 1$) was studied in tensile experiments. A set of high-temperature properties, which can be considered as record-breaking ones among the known shape memory materials, is obtained. In particular, a giant value of TWSME strain equal to about 9% in the vicinity of 300°C is achieved by the proper mechanical training of the samples. The effects observed in this work are consistent with the concept of martensite destabilization (rejuvenation).

The results of this work are also important from a practical point of view. Alongside a significant thermal actuation in high-temperature applications with a large work output, one can anticipate that the actuating element preliminarily trained for a two-way shape-memory effect might exhibit giant magnetic field-induced strains at ambient temperature, due to the detwinning of the non-modulated martensite biased by the internal stress in its rejuvenated state.

Acknowledgements

The financial support from the Department of Education, Basque Government (Project No. IT-347-07) and the Spanish Ministry of Education and Science (Project No. MAT2008 06542-C04-02) is acknowledged. The authors are grateful to V.A. Lvov and P. Mullner for stimulating discussions.

References

1. V.V. Kokorin and V.A. Chernenko. *Phys.Met. Metall.* 68 (1989) 111.
2. V. A. Chernenko, V. L'vov, J. Pons and E. Cesari. *J.Appl. Phys.* 93,2394 (2003).
3. R. C. O'Handley and S. M. Allen, in *Encyclopedia of Smart Materials*, edited by M. Schwartz. Wiley, New York, 2002.
4. *Advances in Shape Memory Materials. Ferromagnetic shape memory alloys*, edited by V. A. Chernenko. TTP, Switzerland .Mat. Sci. Forum, 583 (2008).
5. V. A. Chernenko, E. Cesari, V. V. Kokorin, and I. N. Vitenko. *Scr. Metall. Mater.* 33, 1239 (1995).
6. Y. Li, Y. Xin, C. Jiang, and H. Xu. *Scripta Mater.* 51,849(2004).
7. C. Seguí, E. Cesari, J. Font, J.Muntasell, and V.A. Chernenko. *Scripta Mater.* 53, 315(2005).
8. Y. Li, C. Jiang, and H. Xu. *Mater. Sci. Eng. A*438–440, 978 (2006).
9. H. Xu, Y. Li, and C. Jiang. *Mater. Sci. Eng. A*438–440, 1065 (2006).
10. Y. Xin, Y. Li, L. Chai, and H. Xu. *Scr.Mater.* 54, 1139(2006).
11. C. Seguí, J. Pons, and E. Cesari. *Acta Mater.* 55, 1649 (2007).
12. E. Cesari, J. Font, J. Muntasell, P. Ochín, J. Pons, and R. Santamarta. *Scr. Mater.* 58, 259 (2008).
13. Y. Xin, Y. Li, L. Chai, and H. Xu. *Scr. Mater.* 57, 599 (2007).
14. K.Otsuka and C.M. Wayman, *Shape memory materials*, Cambridge University Press, Cambridge, 1998.
15. M. Ohtsuka, M. Matsumoto, and K. Itadaki. *J. of Intelligent Mater. Systems and Structures* 17, 1069 (2006).
16. F. Xiong and Y. Liu. *Mater. Sci. Eng. A* 432, 178 (2006).
17. W. H. Wang, G. H. Wu, J. L. Chen, C. H. Yu, S. X. Gao, W. S. Zhan, Z. Wang, Z. Y. Gao, Y. F. Zheng, and L. C. Zhao. *Appl. Phys.Lett.* 77, 3245 (2000).
18. L. Straka, O. Heczko, V. Novák, and N. Lanska. *J. Phys.IV France* 112, 911 (2003).
19. J. D. Callaway, R. F. Hamilton, H. Sehitoglu, N. Miller, H. J. Maier, and Y. Chumlyakov. *Smart Mater. Struct.* 16, 108 (2007).
20. E. Cesari, V.A. Chernenko, V.V. Kokorin, J. Pons, and C. Segui. *Acta Mater.* 45, 999 (1997).
21. V. A. Chernenko, E.Villa, V.A. L'vov, S. Besseghini, and J.M. Barandiaran. *Acta Mater.* Submitted.
22. V. A. Chernenko, S. Besseghini, E. Villa, A. Gambardella, and J. I. Pérez-Landazabal. *Appl. Phys. Lett.* 90, 201914 (2007).
23. K. Oikawa, R. Saito, K. Anzai, H. Ishikawa, Y. Sutou, T. Omori, A. Yoshikawa, V.A. Chernenko, S.Besseghini, A. Gambardella, R.Kainuma, and K. Ishida. *Mater. Trans.* 50, 934 (2009).
24. V.A. L'vov, A. Kosogor, O. Söderberg, and S.-P. Hannula. *Mater. Sci. Forum* 13, 635 (2010).